Design of Line Start Permanent Magnet Synchronous Motor using Hybrid Analytical Approach based on Reluctance Network

Hamza Farooq[1], Nicolas Bracikowski [2], Patricio La Delfa[1], and Michel Hecquet[1]

[1]L2EP, Univ. Lille, Arts et Metiers Institute of Technology, Centrale Lille, Junia, ULR 2697 - L2EP, Lille, France
[2]University of Nantes, IREENA 44600 Saint Nazaire, Nantes, France

Line start permanent magnet synchronous motor LSPMSM offers an efficient solution for direct-start applications, serving as a viable replacement for induction motors. Designing LSPMSM involves two key requirements: 1) enabling self-start capability, and 2) delivering sufficient synchronous torque. In this study, a hybrid analytical approach is proposed to evaluate the performance of LSPMSM in both transient (starting) and steady-state (synchronous regime) conditions. To determine design parameters such as back electromotive force (EMF) and magnetizing d-q synchronous reactance, a reluctance network (RN) methodology is used. The off-load RN aids in calculating the back EMF, while the on-load RN is utilized to determine the d-q axis inductances. This approach allows rapid estimation of synchronous torque, ensuring steady-state performance and dynamic speed for assessing the starting response. To validate the findings, the analytically computed results are compared with calculations based on a 2D finite element method (FEM). The developed analytical tool offers valuable insights into the starting and steady-state performance of PMSMs with reduced computational time.

***Index Terms*— Reluctance Network, Line Start Permanent Magnet Synchronous Motor, Transient Analysis, Parametric Study.**

I. Introduction

To replace less efficient induction machines (IM) in direct-start applications, a high-efficiency IE4 class self-starting motor is required. For this purpose, by combining IM and permanent magnet synchronous motor (PMSM) a new technology named line start permanent magnet synchronous motor (LSPMSM) is being introduced in recent years [1]. LSPMSM contains a stator similar to IM and a rotor containing permanent magnets and a squirrel cage. The rotor bars in LSPMSM allow the self-start while the rotor magnets synchronize the motor at a constant speed to function as a PMSM. The permanent magnets inside the rotor provide synchronous torque and reduce the current consumption, which increases efficiency. The design complexity of LSPMSM lies in its rotor design, as the sizing of magnets and bars in the rotor hugely impact the performance. The bars impact the starting performance and during the synchronous regime, its role is insignificant. Whereas, the magnets play a significant role during the synchronous state by providing the synchronous torque. The magnets also impact the starting performance and the synchronizing ability of LSPMSM [2]. Therefore, a trade-off between bar and magnet size is required while designing LSPMSM.

In the literature, several studies are done on the modeling and design of LSPMSM. A reluctance network (RN) based analytical approach is used in recent studies [3]–[5] to compute airgap flux density. The magnetizing d-q inductances were calculated using different methods. In [3], the inductances were calculated by FEM while in [4] it was calculated using the Magnetic Islands method. However, there is a lack of comprehensive procedure which computes the design parameters (Back EMF and magnetizing inductances) using RN. To enhance the existing analytical approach, an extensive parametric study of the rotor magnet and bars is performed in this work. This study is the continuation of the work presented in [6], [7].

This study first calculates the design parameters using the RN methodology. The design parameters (E, X_d, X_q) are then validated using the FEM for a range of design variables to assure the robustness of the RN. The advantage of RN is that it shows the impact of each reluctance component of rotor on the air-gap flux density. The leakage flux through each rotor component is easily predicted. Therefore, the RN allows to understand the machine's behavior in detail. On the other hand, the FEM provides an accurate machine performance but it is difficult to have a mathematical relation that explicitly presents the magnetic circuit.

Secondly, this work presents a parametric analysis for both starting and steady-state performance. The steady-state performance parameter is synchronous torque while the starting performance parameter is rotor speed. The stable operation limits of the LSPMSM are found using the mechanical transient. The starting time of LSPMSM is used as the performance parameter for synchronization.

The current density in the bars is considered uniform in the FEM simulations and analytical model. Therefore, the skin effect on the rotor resistance and consequently the effect on the starting torque is not considered. In this study the LSPMSM is studied for pump application $T_{load} = k\,\omega^2$, there is no requirement for high starting torque. High asynchronous torque is required near the synchronous speed. In this particular case, the precise estimation of starting torque is not required. An extensive analysis of the effect of rotor bar on the starting performance is provided using the average toque steady-state model and the instantaneous transient model. The transient model is used to observe the starting performance of the studied design under mechanical constraints. It also provides the starting time of LSPMSM design which is a parameter to determine the self-starting ability. Whereas the average torque model allows to quickly find the cage torque at a specific rotor speed (slip). This asynchronous torque estimation provides key information about the required rotor bar size to reach a certain asynchronous torque at a given slip. Therefore, this work deals with the design complexity of the LSPMSM rotor by providing a rapid estimation of the starting and steady-state performance.

II. RELUCTANCE NETWORK METHODOLOGY

The procedure to calculate Back EMF E and reactance X_d, X_q using RN is presented in [6], [7]. All the mathematical formulations of reluctances and simplifications are discussed in detail. An off-load RN with only magnets as an excitation is used to calculate Back EMF E. The flux distribution and corresponding RN of the series magnet LSPMSM is presented in Fig. 1. For d-q reactance, the separate d and q axis simplified RN are devised with stator current as an excitation. The whole procedure is implemented on the studied prototype series LSPMSM shown in Fig. 1. The saturation effect in the high flux density region such as the flux bridge is considered using the hypothesis of saturated flux bridge. The reluctance of flux bridge is used with permeability as an air with a constant flux source in parallel. This simplification makes all the reluctance components linear, which allows to simplify the RN and define a mathematical relation to compute the airgap flux density. Using the analytical relation of flux density, the back EMF is calculated in [7].

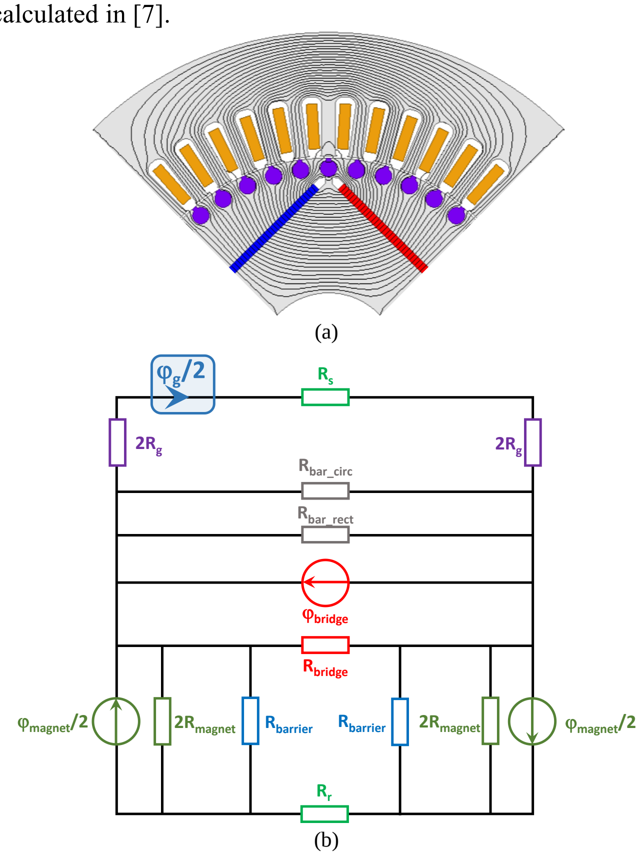

Fig. 1 Studied 4 pole LSPMSM machine: (a)Flux lines in open circuit condition (b) simplified off load reluctance network.

Similarly, the RN is used to compute the magnetizing d-q inductances. The separate flux distribution and RN for the d and q axis are presented in [6]. The inductances calculated by the RN methodology are precise as compared to those computed by analytical expressions. Once the three parameters (E, X_d, X_q) are estimated the synchronous performance of the LSPMSM is evaluated.

III. STARTING AND STEADY STATE MODELLING

A. Steady State Characteristics

As the LSPMSM functions as a PMSM after the synchronization, its steady-state performance parameter is the torque at the synchronous speed defined by (1). It contains magnet and reluctance components. For the surface magnet LSPMSM the torque constitutes only the magnet torque component. δ is the load angle between E and applied voltage V. It depends on the rotor position. During the steady-state δ becomes constant and attains a value that provides the synchronous torque to drive the load torque.

$$T_{sync} = \underbrace{\frac{3p}{\omega}\frac{E\,V}{X_d}\sin\delta}_{T_{magnet}} + \underbrace{\frac{3p}{\omega}\frac{V^2}{2}\left(\frac{1}{X_q}-\frac{1}{X_d}\right)\sin 2\delta}_{T_{reluctance}} \quad (1)$$

B. Transient characteristics

For LSPMSM, the transient state is the starting of the motor before the motor gets synchronized at the synchronous speed. The equivalent electric circuit (EEC) of LSPMSM in the d-q model from the literature [4] is used to determine the instantaneous speed and torque response of the LSPMSM. The mechanical transient of the speed and torque is calculated by (2)-(3).

$$T_{em} = \frac{3N_p}{4}\left(\underbrace{\left[(L_d - L_q)i_{ds}\,i_{qs}\right]}_{Reluctance\ Torque} + \underbrace{\left[L_{md}i'_{dr}i_{qs} - L_{mq}i'_{qr}i_{ds}\right]}_{Induction\ Torque} + \underbrace{\left[\Psi'_m i_{qs}\right]}_{Magnet\ Torque}\right) \quad (2)$$

$$\omega_r = \frac{1}{J}\int (T_{em} - T_{load} - B\omega_r) \quad (3)$$

IV. SENSITIVITY ANALYSIS

A. Magnet Size variation

The robustness of the RN approach is performed by performing a variation of the design variables and observing the impact on the design parameters of the LSPMSM. Two rotor components, magnets which impact steady-state performance and bars which affect the starting performance are selected for variation.

TABLE 1
PARAMETRIC STUDY ON PERMANENT MAGNET SIZE

		Back EMF E (V)		X_d (Ω)		X_q (Ω)	
Design Variable		RN	FEM	RN	FEM	RN	FEM
	(mm)						
w_m	30	104	95	13.9	15.5	28.7	28.9
	35	121	107	13.8	15.5	28.7	28.9
	40	138	125	13.8	15.5	28.7	28.9
	45	156	142	13.8	15.5	28.7	28.9
	50	173	165	13.9	15.5	28.7	28.9
	70	231	230	14.6	15.5	28.9	29.2
h_m	1.5	212	193	16.5	18.08	28.9	29.6
	2	229	220	15.31	16.63	28.8	29.1
	2.5	231	230	14.64	15.5	28.7	28.9
	3	250	248	13.5	12.3	28.5	29
	5	270	265	12.2	10.5	28.2	29.2

The analytically computed results are verified using the 2D FEM as presented in TABLE 1. The RN was devised from the initial design (w_m =70mm, $h_m = 2.5mm$). For a range of magnets dimension closer to the initial design, the RN provides acceptable precision. Whereas large deviation in the magnet dimensions from the initial design leads to imprecise calculation of E, X_d, X_q. The simplified RN used in this study considers the variation of the design variables but it does not consider the variation of saturation effect. Therefore, a large variation from the initial design leads to imprecise results.

Once the RN based methodology is validated by FEM. The calculated design parameters are utilized in the steady-state model (1) to determine the synchronous torque to cost ratio as presented in Fig. 2. The total cost of the material used in the motor is used as the cost factor. The increase of magnet surface area increases the maximum synchronous torque. To avoid large magnet size and consider the cost effect, the response surface depicts the suitable magnet dimensions.

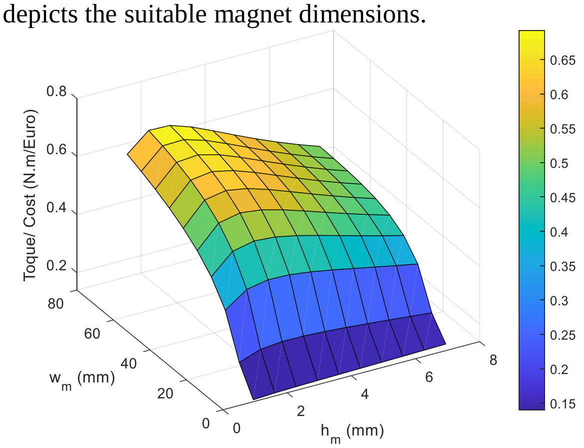

Fig. 2 Parametric study to observe the impact of magnet size on the Torque/Cost ratio.

B. Rotor bar size variation

The effect of rotor bar variation is considered firstly by the average torque model of the steady-state asynchronous machine. The asynchronous torque in function of the slip is used as in (4). TABLE 2 presents the effect of a gradual increase in rotor bar radius. The increase in bar radius decreases the rotor resistance. r_{bar} is the radius of the rotor bar circle, for simplicity purpose only r_{bar} variation is presented in this study. In the $T_{asyn}(0.10) = T_{90}$ is the condition near the synchronous speed while T_{start} is the condition at s=1. Depending upon the required application, starting torque could be designed to be maximum at a specific slip. In this study the pump application is focused therefore, the T_{90} should be higher than the load torque $T_{load} = 47\ N.m$. A fast estimation of the required resistance can be done by the derivative of (4). It provides the value of rotor resistance to achieve the maximum asynchronous torque for a certain slip.

$$T_{asyn}(s) = \underbrace{\frac{3pV^2\frac{R'_r}{s}}{\omega\left[\left(R_s + \frac{R'_r}{s}\right)^2 + (X_{ls} + X'_{lr})^2\right]}}_{T_{cage}}, \quad (4)$$

$$\frac{dT_{asyn}}{dR'_r} = 0$$

To assure the self-starting of LSPMSM, the calculated design parameters are utilized in (2)-(3) and speed versus time response is found. As the rotor bar size significantly impacts induction torque, the rotor bar size is varied to observe its effect on the rotor speed.

TABLE 2 Rotor bar dimensions and the design parameters

r_{bar}	R'_r	X'_{lr}	i_{start}	T_{start}	T_{90}
(mm)	(Ω)	(Ω)	(A)	(N.m)	(N.m)
1	6.07	0.7624	32.26	120.72	16.38
1.25	4.31	0.769	41.71	143.32	22.82
1.5	3.19	0.775	50.64	156.43	30.45
2	1.93	0.789	64.9	154.8	48.435
2.45	1.34	0.80115	72	133.6	66.65
3	0.93	0.8158	78	109	89.43
3.2	0.83	0.82119	79	101.34	97.40

Fig. 3 presents the impact of r_{bar} variation on the speed. For the nominal operating conditions, the smaller r_{bar} does not start the LSPMSM. Whereas the larger r_{bar} smoothly starts the machine due to its ability to provide induction torque higher than the load torque before the synchronous regime.

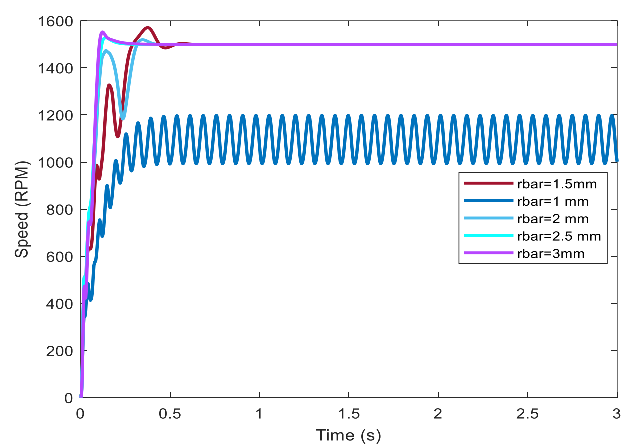

Fig. 3 Impact of rotor bar size variation on the starting of LSPMSM.

The rotor bar size also impacts the synchronizing ability under the loaded condition. To verify the ability to sustain an overload condition the design is applied with a load torque higher than the nominal value. Fig. 4 presents that the smaller bar does not provide sufficient asynchronous torque to help the synchronization. While the $r_{bar} = 3\ mm$ allows to start and synchronize although it takes high time to start. Therefore, increasing the rotor bar slot increases the capacity of the LSPMSM to synchronize the higher load torque.

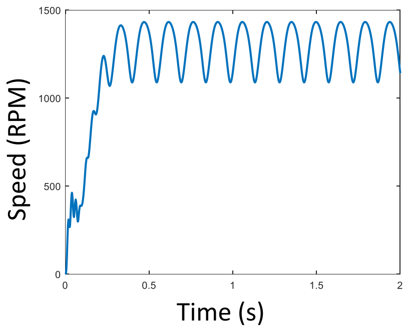

(a)
$r_{bar} = 2\,mm,$
$T_{load} = 55\,N.m$

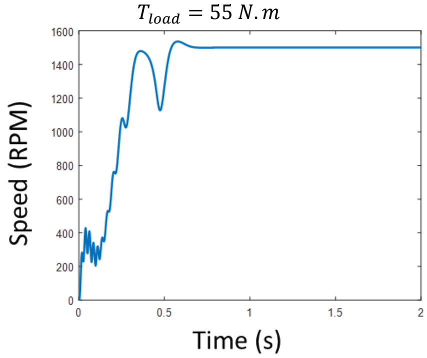

(b)
$r_{bar} = 3\,mm,$
$T_{load} = 55\,N.m$

Fig. 4 Effect of rotor bar size on the load capacity.

C. Effect of magnets on the synchronizing ability of LSPMSM

A criterion to measure find the synchronization ability of a given design is determined using a rotor speed. When the rotor speed is $\pm 2\%$ of the synchronous speed, the LSPMSM is considered synchronized. The time a certain design takes to validate this criterion is regarded as the starting time. The small magnet size provides low synchronous torque, LSPMSM takes high time to synchronize. The designs with moderate magnet size provide sufficient torque, the motor starts rapidly. Beyond a certain range of magnet size, an excessive synchronous torque is produced. This excessive torque is advantageous for the synchronous state but for the starting period it creates a magnet breaking torque, slowing down the start. Therefore, a region of motor designs which start smoothly is predicted in Fig. 5 using the analytical approach. Starting time for each design is simulated using analytical model which allows to do it fastly, 400 simulations were performed in 25 minutes. While the finite element method (FEM) simulation for one design takes 1 hour 20 minutes, because of time step magneto dynamic analysis. Therefore, the advantage of analytical model lies in fast estimation of suitable design range in the pre-design stage.

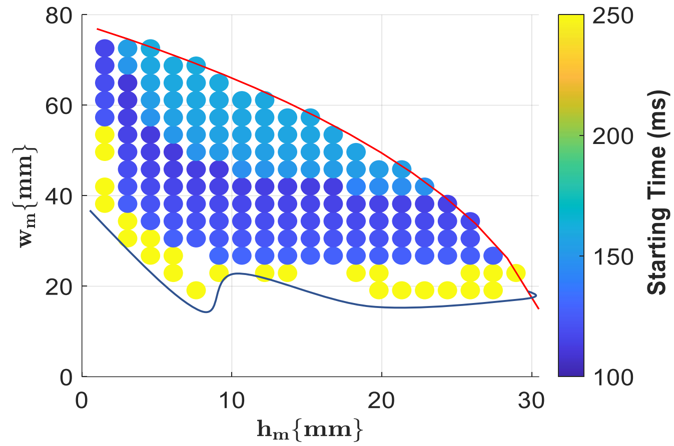

Fig. 5 Impact of magnets size on the synchronization of LSPMSM.

V. Conclusion

The presented approach analytically performed parametric analysis on the rotor magnet and rotor bar dimensions. Further, the effect of magnet and bar size variation on the steady-state and starting performance of LSPMSM is observed. It is found that the rotor magnet size is vital to the ability of LSPMSM to operate with high a Torque/Cost ratio. The magnets also impact the synchronizing time of the LSPMSM. The rotor bars are only important during the starting phase. A good combination of bars and magnets provides a stable and smooth start and operation of LSPMSM.

An experimental study is currently in progress to validate the analytical approach. In future studies a comparison of LSPMSM performance found analytically, simulated by FEM, and measured experimentally will be provided. The analytical model presented in this study will be used to design other topologies to verify the robustness of the method. Further effects will be considered in future studies to enhance the precision of the developed tool.

References

[1] R. F. McElveen, R. A. Holub, and W. E. Martin, "Replacing Induction Motors With Caged-Rotor Permanent Magnet Motors: Application Considerations and Cost Analysis," IEEE Ind. Appl. Mag., no. August, pp. 67–75, 2020.

[2] A. Hassanpour Isfahani and S. Vaez-Zadeh, "Line start permanent magnet synchronous motors: Challenges and opportunities," Energy, vol. 34, no. 11, pp. 1755–1763, 2009.

[3] A. Waheed and J. S. Ro, "Analytical Modeling for Optimal Rotor Shape to Design Highly Efficient Line-Start Permanent Magnet Synchronous Motor," IEEE Access, vol. 8, pp. 145672–145686, 2020.

[4] M. M. Ghahfarokhi, A. D. Aliabad, S. T. Boroujeni, E. Amiri, and V. Z. Faradonbeh, "Analytical modelling and optimisation of line start LSPM synchronous motors," IET Electr. Power Appl., vol. 14, no. 3, pp. 398–408, 2020.

[5] J. G. Lee and D. K. Lim, "A Stepwise Optimal Design Applied to an Interior Permanent Magnet Synchronous Motor for Electric Vehicle Traction Applications," IEEE Access, vol. 9, pp. 115090–115099, 2021.

[6] H. Farooq, N. Bracikowski, P. La Delfa, and M. Hecquet, "Modelling of Starting and Steady-State performance of Line Start Permanent Magnet Synchronous Motor using Reluctance Network," in 2022 International Conference on Electrical Machines (ICEM), pp. 226–231, 2022.

[7] H. Farooq, N. Bracikowski, P. La Delfa, and M. Hecquet, "Estimation of Steady-State Torque of Line Start Permanent Magnet Synchronous Motor using Reluctance Network Approach," Electrimacs, 2022, to be published.